

## APPLICATION OF LOW-COST MAGNETIC FIELD AND ACCELERATION SENSORS IN DIAGNOSTICS OF LARGE-SIZE STRUCTURES

Przemysław SZULIM, Jędrzej MAĆZAK, Krzysztof ROKICKI, Kamil LUBIKOWSKI

Warsaw University of Technology, Faculty of Automotive and Construction Machinery Engineering  
Narbutta 84, 02-524 Warszawa, Poland, e-mail: [p.szulim@mechatronika.net.pl](mailto:p.szulim@mechatronika.net.pl), [jma@mechatronika.net.pl](mailto:jma@mechatronika.net.pl),  
[k.rokicki@mechatronika.net.pl](mailto:k.rokicki@mechatronika.net.pl), [klubikowski@mechatronika.net.pl](mailto:klubikowski@mechatronika.net.pl)

### Summary

The paper presents the possibilities of using low-cost magnetic and acceleration sensors in diagnostic systems of large-scale structures made of ferromagnetic materials. It covers typical problems associated with their use as well as the review of commercially available low-cost solutions. A specially designed magnetic sensor equipped with a CAN interface, which allows for connecting a number of transmitters into a measuring network, were tested during the experiment.

Keywords: diagnosis, magnetic sensors, MEMS sensors, diagnostic systems.

### ZASTOSOWANIE NISKOBUDŻETOWYCH CZUJNIKÓW POLA MAGNETYCZNEGO I PRZYSPIESZEŃ W DIAGNOSTYCE KONSTRUKCJI WIELKOGABARYTOWYCH

#### Streszczenie

W pracy przedstawiono możliwość wykorzystania niskobudżetowych czujników pola magnetycznego i przyspieszeń w systemach diagnostyki konstrukcji wielkogabarytowych wykonanych z materiałów ferromagnetycznych. Przedstawiono typowe problemy występujące podczas ich użycia oraz dokonano przeglądu dostępnych na rynku tanich rozwiązań. W przeprowadzonym eksperymencie przetestowano specjalnie opracowane przetworniki pola magnetycznego wyposażone w interfejs CAN pozwalający na łączenie szeregu przetworników w sieć pomiarową.

Słowa kluczowe: diagnostyka, czujniki magnetyczne, czujniki MEMS.

## INTRODUCTION

Use of magnetic information for diagnosing the condition of structures is not a new idea. There exist numerous methods and their commercial applications. Majority of them required are the so-called active methods, as they offer easier interpretation of results. Passive methods, which only rely on registration of changes in the magnetic field surrounding a structure, form a separate group. Such a passive method, along with research results, is described in [1] and [2]. Though the work related to this class of methods has not been completed yet, the results which have been obtained so far are often very promising. Some examples were presented in [3] where the passive magnetic methods were used during the experiment for monitoring the behavior of a large-size truss which was subjected to heavy loads. The examined truss corresponds to a structural element of steel warehouses. The truss was subjected to the loads which were similar to the loads occurring in actual facilities. The results of the experiment are presented in more detail in the further part of the article in connection with the description of magnetic field converters.

## 1. REVIEW OF SENSORS

In this chapter a review of low-budget magnetic field converters as well as the most interesting solutions, characterized by relatively good technical parameters and low price will be presented. The sensor described as the last one has been designed for the purpose of development of the diagnostic methods which rely on magnetic field measurements.

The MAG3110 sensor is an integrated, digital, tri-axial magnetic field sensor manufactured by Freescale. It has single measuring range and 8 sampling frequencies ranging from 0.63Hz to 80 Hz. The measuring range of the sensor is +/-1000uT, which in the case of a built-in 16-bit converter enables achievement of the resolution of 0.03uT. It is worth to note that the signal to noise ratio is very low for this sensor, as shown on the product sheet [4]. However, lack of information regarding the structure of the analogue part of the sensor suggests that not much attention was devoted to aliasing phenomena. The authors' experience with this sensor shows that the noise level is in fact lower than in the case of LSM303 sensor (described in the

further part of the article). The integrated electronic circuit of this digital sensor makes sure that the analog signal sampling is performed with pre-programmed frequency. Measurement data are available via the I2C bus. What is also worth noting there are separated power supplies for the analog and the digital parts. Thanks to this separation, the level of noise has been reduced in the measured signal. Temperature measurement of the semiconductor structure of the system is also available. The information regarding the temperature can be used for assuring temperature-wise adjustment of such parameters as sensitivity or bias, that is the parameters which are sensitive to temperature changes in a lesser or greater degree.

Another noteworthy sensor is the analog sensor which relies on the effect of giga-magneto-resistance. NVE Corporation manufactures numerous sensors. One of them, having the code AAH002 [5], is characterized by relatively high sensitivity and ability to operate in uni-polar configuration. It is undoubtedly the drawback but at the same time the characteristic feature of sensors of this type. The sensor can measure magnetic fields correctly only in the ranges from  $-$  to 0 or from 0 to  $+$  values. It is unable to perform measurements in the range from  $-$  to  $+$  values. At least the measurements cannot be performed in a simple measuring system. The sensor contains a bridge composed of measuring elements (Fig. 1). The voltage at the output of the bridge changes proportionally to the value of the applied magnetic field. The fact that the sensor is an analog one allows for building of own set of amplifiers and anti-aliasing filters, enabling much higher sensitivity and better elimination of measurement noise. What is more, this solution offers a theoretical possibility of constructing a low-cost differential magnetic field sensor.

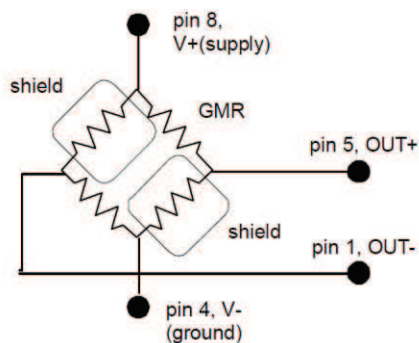


Fig. 1 Electrical diagram of AAH002 sensor [5]

Another interesting device is a RM3000 geomagnetic sensor offered by PNI Corporation [6].

This relatively cheap sensor relies on the hysteresis effect which occurs in the ferromagnetic core. The company supplies separate analog sensors as well as ASIC systems which are integrated analog-digital sets.

Analyzing available sensors, it is worth considering a ready integrated solution since analog sensors require quite complex electronic circuit to obtain a measurement. The sensors are characterized by a typical measuring range, similar to the ones mentioned earlier. Relatively high resistance to temperature changes is undoubtedly an advantage of this sensor. It is a very important feature, since there are numerous applications which require the sensors to operate in an environment with varying parameters, such as temperature, humidity, etc. Insensitivity of a sensor to changes of these parameters leads to reduction of measurement errors.

An acceleration sensor which deserves more attention from among the wide range of acceleration converters is the ADXL001 (Fig. 2).

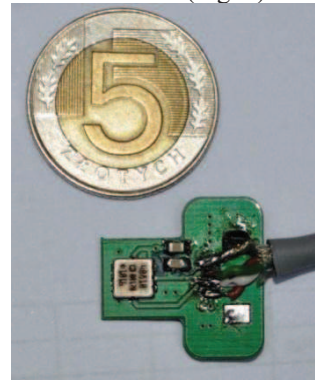


Fig. 2 Acceleration sensor ADXL001 on a test board

ADXL001 is a single-axis acceleration sensor from Analog Devices [7]. Depending on the version, the sensor can measure acceleration in the range of  $\pm 70g$ ,  $\pm 250g$  and  $\pm 500g$ . The sensor relies on MEMS technology. It is also an analog sensor. Since the sensor is characterized by quite extensive band of 0-33kHz, thus it can be used in various types of vibration tests as well as in modal analysis.

The acceleration and magnetic field sensor board (Fig. 3) has been developed for the needs of the experiment aimed at testing the possibilities of using the passive magnetic methods for diagnosis of structures (Fig. 3). The board consists of several principal parts. The main measuring element is an integrated LSM303 tri-axial accelerometer combined with a tri-axial magnetometer sensor. Basic technical parameters of the sensor can be found in the product sheet [8].

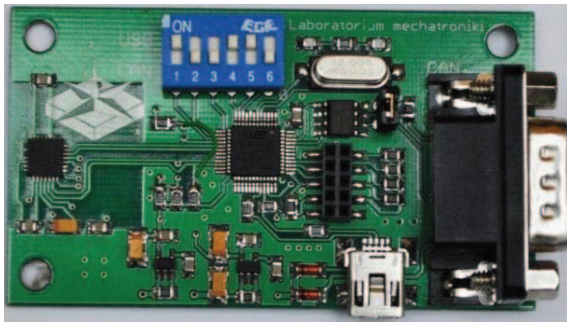


Fig. 3 Magnetic field and acceleration sensor board

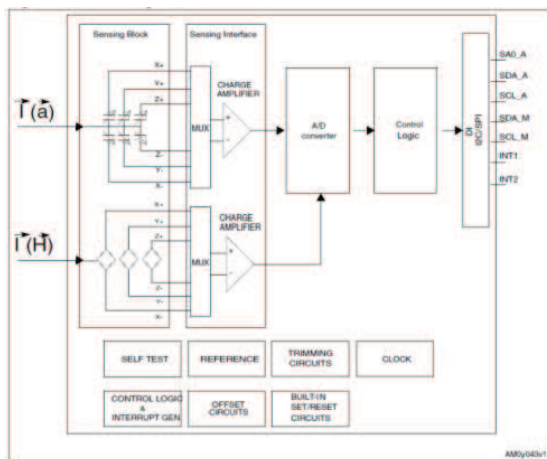


Fig. 4 Internal diagram of the LSM303 sensor [8]

The signal from the measurement bridges undergoes preliminary amplification and processing with the use of a 12-bit A/C converter. The signal becomes available to the master computer/microcontroller via the I2C bus. It is a typical bus for communication between two devices operating at a close distance from each other. It is not suitable for transmitting data over longer distances and that is why apart from communicating with the LSM303 sensor, the developed sensor board is also involved in transmitting data to the CAN bus. The magnetic sensor has 7 sensitivity settings. In the variant with the biggest sensitivity the sensor carries out measurements in the range of  $\pm 1.3g$ , which, when combined with the sensitivity of the converter, means measurement accuracy at the level of  $1mg$ . The last variant is the variant with the broadest range which enables magnetic field measurements in the range of  $\pm 8.1g$ . Frequency of measurements is the issue which is important in the case of measurements of this type. Seven sampling speeds can be set for this sensor ranging from  $0.75Hz$  to  $70Hz$ . One should note that frequency of sampling is not synonymous with the necessity of reading the data from the sensor at the same rate. The manufacturer also informs that as the sampling frequency changes, so does the anti-aliasing filter band. It is a very important issue which, as it turned during the tests, has not been solved well by the manufacturer. While measurements are performed

on structures, there often happen situations where apart from the static magnetic field, which is associated with the earth's magnetic field and the magnetic field generated by the structure itself, there appears a magnetic field component which is characterized by significant frequency and often associated with the network noise. In order to properly filter off the noise it is necessary to create registration conditions which fulfill the Nyquist criteria. As it turned out the manufacturer did not provide sufficiently good anti-aliasing filters, which oftentimes caused numerous problems. The analog track is undoubtedly the weak side of the solution. An important feature of the LSM303 sensor is the fact that it has been factory-calibrated. The calibration concerns sensitivity of the axis, influence of temperature on the sensor's axis and offset. In this very case, offset is understood to be a certain permanent component which appears in the measured signal. It is worth remembering that calibration concerns the LSM303 only. This sensor is embedded in a device and due to the presence of soft and hard ferromagnetic materials it requires recalibration. This issue is very important, however due to its extensive nature it goes beyond the framework of the present article. It is also worth noting that the axis of the sensor need not necessarily be perpendicular while the errors associated with the axis not being perpendicular to one another may even be in the range of several degrees. These items are also the parameters which are subject to calibration. The manufacturer's solution, which gives a user the possibility of selecting the sensitivity, offers, on the one hand, bigger flexibility but on the other it generates a real calibration issue, since calibration would have to be done separately for each of the ranges.

The possibility of measuring the acceleration is an interesting feature of the constructed device. A tri-axial accelerometer, built-in into the LSM303 sensor, has been developed in MEMS technology. Its most important features include: sampling frequency of up to  $1kHz$  (the signal from the accelerometers is only available in digital format), three measurement ranges:  $\pm 2g$ ,  $\pm 4g$ ,  $\pm 8g$ , as well as quite good temperature-related parameters, namely influence of temperature on the stability of sensitivity and influence of temperature on the stability of zero value. Quite a narrow measuring range makes it impossible for the device to be used for e.g. measuring the vibration of structures. However use of the sensor for measuring the deformation of structures presents an interesting application of the device. MEMS-technology-based sensors enable measurement of gravitational acceleration. Similarly as in the case of other types of sensors, the measurement is indirect and it is performed by measuring the force interacting with some standard mass as a result of acceleration. Since the sensor also measures the value of a constant component of acceleration, then while assuming that

the sensor is immobile it is possible to measure the gravitational acceleration. Since its value can be treated as a constant value, thus measurement of the acceleration vector can be used for determining the angle of turn of the sensor. A sensor located in a measurement device and attached to the examined structure, can easily be used for detecting a spot defect (e.g. caused by buckling of its elements). Choice of the angles which describe the variance of the acceleration vector, as seen in the system of the sensor's coordinates, depends on many factors. It is usually best to choose the ones whose interpretation will be easiest and the ones which will later on provide the best information. The below figure (Fig. 5) presents an example of a coordinate system of a sensor, featuring the marked acceleration vector and the two angles describing variance of the vector thus describing the movement of the sensor with regard to a certain straight line which is perpendicular to the earth.

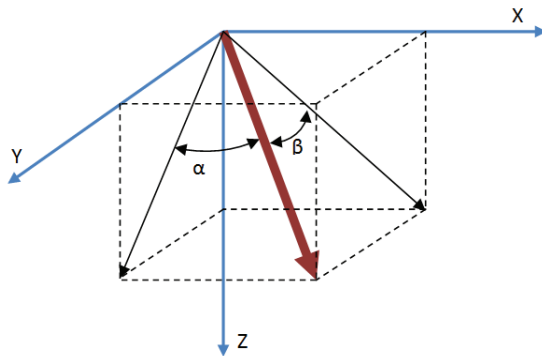


Fig. 5 Coordinate system showing angles of revolution of the sensor

It is worth noting that precision of acceleration measurement achieved for the resolution of the 12 bit ADC converter and its range of 2g is 1 mg. For this data the precision of angle measurement of  $0.05^\circ$  is achieved for small values of angles  $\alpha$  and  $\beta$ . What causes the problem is the measurement noise and that is why it is suggested that analog sensors with an enhanced analog measurement circuit should be used for achieving a more precise measurement.

## 2. CALIBRATION

Characteristic features of low-cost sensors are the big discrepancies of such parameters as sensitivity or zero level (the so-called offset). Hence before the possibilities offered by these sensors are used in practice, they must first undergo calibration. Calibration of sensors is quite complex and it goes beyond the scope of the present article. Only an outline of the process will be presented here, along with the general principle demonstrating the way in which calibration can be performed. The equation presented below describes the easiest model which links the value registered by a sensor to the actual physical value:

$$m_f = s * (m_m - b) \quad (1)$$

The physical value  $\mathbf{m}_f$  is registered by the sensor as  $\mathbf{m}_m$ . Once a certain constant value  $\mathbf{b}$  is subtracted and the result is multiplied by a sensitivity parameter  $\mathbf{s}$ , we arrive at the physical interpretation of measurement  $\mathbf{m}_f$ . In a situation of a measurement performed with the use of a tri-axial sensor, parameters  $\mathbf{b}_i$  and  $\mathbf{s}_i$  are assigned to each axis  $\mathbf{i}$ . The model (1), however, fails to account for non-perpendicularity of the axis. This fact is only addressed by the model (2).

$$m_{f_i} = s_{i1} * (m_{m1} - b_1) + s_{i2} * (m_{m2} - b_2) + s_{i3} * (m_{m3} - b_3) \quad (2)$$

which in the case of tri-axial measurement can be presented by means of a matrix equation (3)

$$\overline{m}_f = S * (\overline{m}_m - B) \quad (3)$$

where S is a matrix with a dimension of 3x3, while B is matrix with a dimension of 3x1. When the sensor is non-linear, then its non-linearity can be approximated by means of a second degree multinomial. In such a case the measurement model can be as presented by equation (4).

$$\overline{m}_f = S * \begin{pmatrix} a_x(m_{mx} - b_x)^2 & m_{mx} - b_x \\ a_y(m_{my} - b_y)^2 & m_{my} - b_y \\ a_z(m_{mz} - b_z)^2 & m_{mz} - b_z \end{pmatrix} \quad (4)$$

Similarly as (1) and (2), the model described by equation (4) can serve as the basis for developing a system of equations for the purpose of determining the unknown factors of matrices S, B and A ( $a_x, a_y, a_z$ ). To solve such a system of equations one needs to use equation (5), i.e. an equation determining the module of a measurement vector which should be a constant value (on the assumption that the vector field has a constant value).

$$|\overline{m}_f| = \sqrt{m_{fx}^2 + m_{fy}^2 + m_{fz}^2} \quad (5)$$

While using equations (4) and (5) it is possible to develop a system of 15 equations, yet it will be impossible to make, in a simple way, a transformation which would enable determining all the coefficients which are sought. It could be done while using e.g. the Newton's algorithm which would bring us closer to the solution. However, it is also worth noting that the results of the measurements which have been obtained while using a tri-axial sensor can be shown on the graph XYZ. In the case of a calibrated sensor the vector should be "sliding" with its vertex on the surface of a sphere. Calibration errors for offset B will result in shift of the center of the sphere, sensitivity-related errors result in emergence of an ellipsoid instead of a

sphere, while the errors associated with skewness of the axis can lead to either a turn of the ellipsoid or its deformation. Fig. 6 presents a graph with a trace of a magnetic field vector obtained during multiple rotations of the sensor. Such a big number of measurement points is relatively easy to obtain for magnetic field sensors, however in the case of accelerometers, for which measurements have to be made in static conditions (only gravitational acceleration is permitted), such a big number of measurement points would be difficult to achieve.

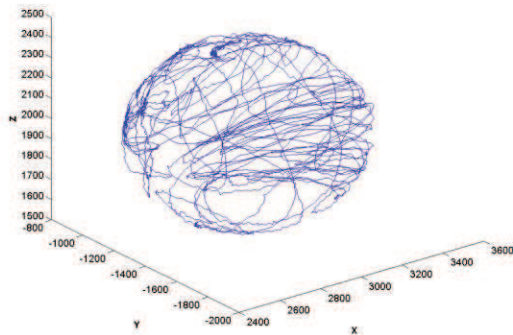


Fig. 6 Measurement data registered by the sensor MAG3110

**3. EXEMPLARY RESULTS OF MEASUREMENTS**

This section presents some of the results obtained during the experiment involving application of load to a steel truss used in the structure of rooftops of warehouses [3]. Numerous measurements were performed during the experiment, such as strain gauge measurements, measurements of deflection with the use of LVDT, modal measurements or measurements of deflection while relying on visual methods. Mainly the measurements involving low-cost sensors will be presented.

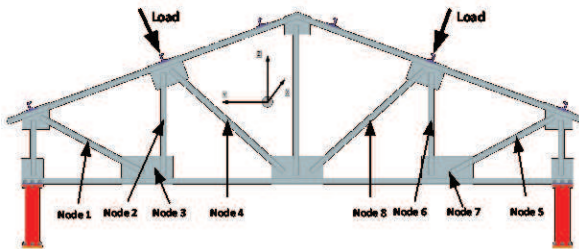


Fig. 7 Location of sensors

In the first phase of the measurement, the examined structure is subjected to a gradually increasing load produced by two hydraulic actuators generating force from 0 to 35 kN each (Fig. 7). The

structure was damaged due to buckling when the load reached around 35 kN.

Fig. 8 presents the graph showing the changes of the angle  $\beta$  during the experiment. The upper graph shows the input force while the lower graph contains the results of measurement of the angles in three measurement nodes. It should be noted that the 10 so-called measurement nodes were placed on the structure, with measurements conducted in these nodes while using strain gauges and magnetic sensors as well as accelerometers.

Figure 8 shows that during the first phase of the load application on the construction, when the force changed in the range from 10 to 35kN, the angle of turn, as registered in respective nodes, practically did not change.

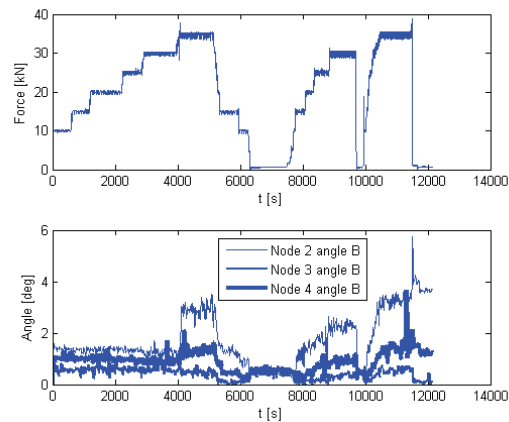


Fig. 8 Influence of the load on angle  $\beta$

It is only the buckling that brought a rapid change of readings. The impact of buckling varied, depending on the location of a measurement node on the frame. Once buckling occurred (approx. in the 4000<sup>th</sup> second of the experiment), the load-exerting force had permanent influence on the value of the angle registered by the sensors. The reason was that once the load was released the structure did not return to its original form but remained permanently bent. Subsequent load cycles led to growth or decrease of the structure's deflection, which was registered by the sensors.

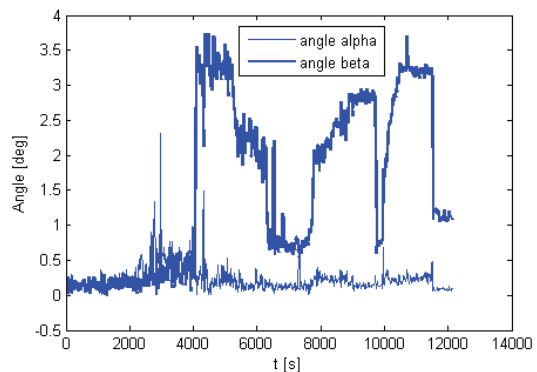


Fig. 9 Change of angles  $\alpha$  and  $\beta$  for node 6 during the experiment

Fig. 9 presents a graph showing the values of angles  $\alpha$  and  $\beta$  in the measurement node no. 6. It can be seen from the graph that angle  $\alpha$  has not changed during the experiment. Due to the nature of the buckling, changes of angle  $\alpha$  were small, that is why we neglected them while presenting the results. Figure 10 presents the results of measurement of angles  $\beta$  for measurement nodes 6,7,8. The impact of buckling is distinctly visible in each case. It should be added that the relatively high value of the measurement noise is associated with the rather poor properties of the filters. Since other additional measurements were performed on the structure's surface during each subsequent phase, thus each case of impact or leaning against the structure was registered by the accelerometers. The target version should be equipped with a filter cutting off higher frequencies of the signal.

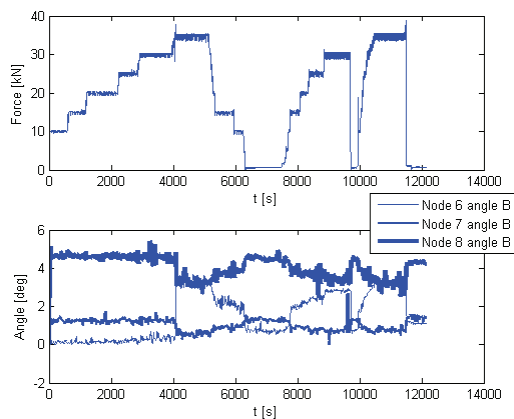


Fig. 10 Impact of the load on change of angle  $\beta$

Figure 11 contains a graph showing changes of the module of the magnetic field's vector during the experiment. The presented results concern the measurement nodes 1-3.

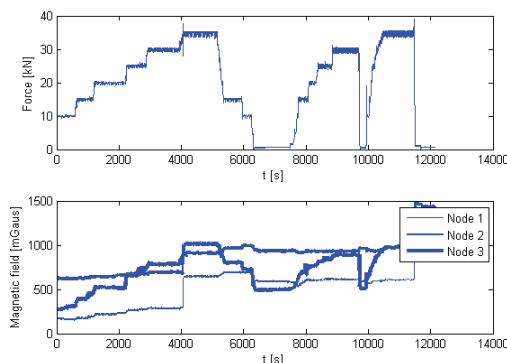


Fig. 11 Change of the module of the magnetic field's vector for the nodes 1,2 and 3

Figure 12 presents the same situation for measurement nodes 5-7. The influence of the load-exerting force, shown in the upper graph, is clearly visible. It can also be seen that occurrence of the defect led to rapid growth of the magnetic field's value.

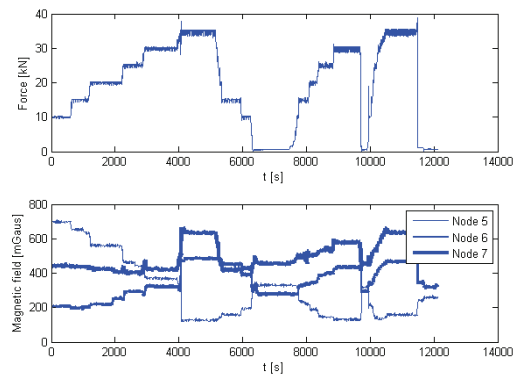


Fig. 12 Change of the module of the magnetic field's vector for the nodes 5,6 and 7

#### 4. CONCLUSIONS

The article presents several selected low-cost magnetic field and acceleration sensors which can be used in diagnostic systems. A review of the sensors is presented while pointing to some of their features. Also an outline of the process of calibration of sensors is presented, along with the results of data registration during an actual experiment. As has been presented above, the sensors provide interesting information which can be successfully used while building diagnostic systems.

#### REFERENCES

- [1] Gontarz S., Radkowski S., *Impact of Various Factors on Relationships Between Stress and Eigen Magnetic Field in a Steel Specimen*, IEEE Transactions on Magnetics, 48(3), 2012
- [2] Gałęzia A., Gontarz S., Jasiński M., Maćzak J., Radkowski S., and Seńko J., *Distributed System for Monitoring of the Large Scale Infrastructure Structures Based on Analysis of Changes of its Static and Dynamic Properties*, Key Engineering Materials, vol. 518, pp. 106–118, 2012,
- [3] Maćzak J., *A Structural Health Monitoring System Based on an Analysis of Changes in the Static, Dynamic and Magnetic Properties of the Structure*, in B.H.V. Topping, (Editor), "Proceedings of the Eleventh International Conference on Computational Structures Technology", Civil-Comp Press, Stirlingshire, UK, Paper 86, 2012.
- [4] *Xtrinsic MAG3110 Three-Axis, Digital Magnetometer* [Online]. Available: [http://freescale.com/files/sensors/doc/data\\_sheet/MAG3110.pdf](http://freescale.com/files/sensors/doc/data_sheet/MAG3110.pdf). [Accessed: 01-Dec-2013]
- [5] *AA and AB-Series Analog Sensor*. NVE Corporation. [Online]. Available: [http://www.nve.com/webstore/catalog/redirect.php?action=url&goto=www.nve.com%2FDownloads%2Fanalogue\\_catalog.pdf](http://www.nve.com/webstore/catalog/redirect.php?action=url&goto=www.nve.com%2FDownloads%2Fanalogue_catalog.pdf) [Accessed: 01-Dec-2013]

- [6] *RM3000 / RM2000* | PNI Sensor Corporation [Online]. Available: <http://www.pnicorp.com/products/RM3000-RM2000#Features>. [Accessed: 01-Dec-2013].
- [7] *ADXL001 datasheet and product info* | High Performance Wide Bandwidth iMEMS® Accelerometer | MEMS Accelerometers | Analog Device [Online]. Available: <http://www.analog.com/en/mems-sensors/mems-accelerometers/adxl001/products/product.html>. [Accessed: 01-Dec-2013].
- [8] *LSM303DLM Sensor module: 3-axis accelerometer and 3-axis magnetometer - STMicroelectronics* [Online]. Available: [http://www.st.com/web/catalog/sense\\_power/FM89/SC1449/PF251902](http://www.st.com/web/catalog/sense_power/FM89/SC1449/PF251902). [Accessed: 01-Dec-2013].

**Jędrzej MAĆZAK**, PhD is an assistant professor at the Institute of Vehicles of the Warsaw University of Technology. His scientific interests are distributed diagnostic systems, machine diagnostics and methods of analysis of vibroacoustic signals.



**Przemysław SZULIM**, M.Sc., a Ph.D. student in the Institute of Vehicles of Warsaw University of Technology.



**Kamil LUBIKOWSKI**, M.Sc., a Ph.D. student in the Institute of Vehicles of Warsaw University of Technology.



**Krzysztof ROKICKI**, M.Sc., a Ph.D. student in the Institute of Vehicles of Warsaw University of Technology.

